

Lawrence Berkeley National Laboratory

Recent Work

Title

WAVELENGTH-MODULATION SPECTRA OF SOME SEMICONDUCTORS

Permalink

<https://escholarship.org/uc/item/6g8604h0>

Authors

Zucca, Ricardo R.L.
Shen, Y.R.

Publication Date

1969-10-01

Submitted to Physical Review

UCRL-19091
Preprint

ly-Z

WAVELENGTH-MODULATION SPECTRA OF SOME SEMICONDUCTORS

RECEIVED
LAWRENCE
RADIATION LABORATORY

NOV 5 1969

LIBRARY AND
DOCUMENTS SECTION

Ricardo R. L. Zucca and Y. R. Shen

October 1969

AEC Contract No. W-7405-eng-48

TWO-WEEK LOAN COPY

*This is a Library Circulating Copy
which may be borrowed for two weeks.
For a personal retention copy, call
Tech. Info. Division, Ext. 5545*

LAWRENCE RADIATION LABORATORY
UNIVERSITY of CALIFORNIA BERKELEY

UCRL-19091
ly-Z

DISCLAIMER

This document was prepared as an account of work sponsored by the United States Government. While this document is believed to contain correct information, neither the United States Government nor any agency thereof, nor the Regents of the University of California, nor any of their employees, makes any warranty, express or implied, or assumes any legal responsibility for the accuracy, completeness, or usefulness of any information, apparatus, product, or process disclosed, or represents that its use would not infringe privately owned rights. Reference herein to any specific commercial product, process, or service by its trade name, trademark, manufacturer, or otherwise, does not necessarily constitute or imply its endorsement, recommendation, or favoring by the United States Government or any agency thereof, or the Regents of the University of California. The views and opinions of authors expressed herein do not necessarily state or reflect those of the United States Government or any agency thereof or the Regents of the University of California.

WAVELENGTH-MODULATION SPECTRA OF SOME SEMICONDUCTORS

Ricardo R. L. Zucca[†] and Y. R. Shen
Department of Physics, University of California
and Inorganic Materials Research Division,
Lawrence Radiation Laboratory
Berkeley, California 94720

ABSTRACT

Wavelength modulation spectra of GaAs, GaSb, InAs, InSb, Ge, and Si at 5, 80, and 300°K are presented. The spectral range extends from 1.75 to 6.0 eV. The results are compared with electroreflectance and thermorelectance data. New structures are found in the spectra of all crystals. With the help of existing band structures of these crystals, all the reflectivity peaks can be consistently assigned to proper critical transitions between the valence and the conduction bands. Values of spin-orbit splittings at several symmetry points can be calculated. Temperature effects on the band spectra are discussed.

[†]Fellow, Consejo Nacional de Investigaciones Cientificas y Tecnicas,
Argentina

I. INTRODUCTION

In recent years, the subject of band structures of semiconductors has again attracted much attention. Theoretically, the introduction of the empirical pseudopotential method¹ has led to a much better understanding of the band structures. Further progress requires improvement on the resolution of empirical spectra. Experimentally, the application of optical derivative spectroscopy to solids has greatly improved the resolution of optical spectra. The results have had strong impact on the recent advance in band structure calculations.

Many different modulation schemes have been invented for derivative spectroscopy. For measurements of reflectivity spectra of solids, electroreflectance,² piezorefectance, thermorelectance,^{6,7} and wavelength modulation⁸ methods have been most successful. In all these schemes except the wavelength modulation method, modulation of the light beam is obtained through application of a direct ac perturbation on the solid, and hence, interpretation of the derivative spectrum depends very much on how the solid responds to the perturbation. Thus, in electroreflectance, we must know how the band structure of the solid changes with an applied electric field. In piezorelectance and thermorelectance, we must know the variation of the band structure as a function of pressure and temperature respectively. Unfortunately, our knowledge on such properties of a solid is generally rather limited. Therefore, the fact that no perturbation on the solid is needed makes the wavelength modulation method most attractive. Since the wavelength modulation spectrum is simply the derivative of the normal spectrum, there is no ambiguity in the interpretation.

However, unlike the other modulation schemes, the wavelength modulation method requires careful construction of the experimental system in order to eliminate the huge background in the derivative spectrum. This background appears as a result of wavelength modulation on the spectra of various optical components in the system. In particular, because of the many narrow spectral lines in the arc source, it is difficult to apply the scheme to the uv region. For this reason, the wavelength modulation method has not been as popular as the other modulation schemes. Work done with wavelength modulation has usually been limited to a narrow region in the visible or near infrared.⁹⁻¹¹

Recently, we have succeeded in constructing a wavelength modulation spectrometer which practically eliminates all the background. On the other hand, the sensitivity of the spectrometer is still as high as $\Delta R/R \cong 10^{-4}$. We have used this spectrometer to obtain derivative spectra of Si, Ge, GaAs, GaSb, InAs, and InSb from 1.75 to 6 eV. In order to resolve fine structures in the spectra, we have made measurements at liquid nitrogen and liquid helium temperatures. In this paper, we would like to present the results of our investigation. While the gross features of our spectra agree with the results of others,^{3,7} new structures and more fine details appear in our spectra, particularly in the uv region.

In the following section, a brief description of the experimental arrangement is first given. Then, in Section III, the wavelength modulation spectra of the six semiconductors at 5, 80, and 300°K are presented. In Section IV, the derivative spectra are analyzed with the help of the existing band structures of semiconductors, various

reflectivity peaks are assigned to proper critical transitions between bands. Emphasis is on the new structures we have observed. Variation of the derivative spectra with temperature is discussed qualitatively.

II. EXPERIMENTAL ARRANGEMENT

A. The Spectrometer

The detailed construction of our wavelength modulation spectrometer will be described elsewhere.¹² Here, we shall give only a brief account of it. Wavelength modulation was achieved through vibration of a mirror in the optical path inside the spectrometer. A double beam method was used to eliminate the background in the derivative spectrum. One beam had its dc and ac outputs proportional to I_0 and $\Delta I_0/\Delta\lambda$ respectively, and the other had outputs proportional to $I_0 R$ and $\Delta(I_0 R)/\Delta\lambda$ respectively, where I_0 is the beam intensity in the absence of the sample, and R is the reflectivity of the sample. Two of the outputs were used to control two feedback loops, making $\Delta I_0/\Delta\lambda = 0$ and $I_0 = \text{constant}$ (or $I_0 R = \text{constant}$). The other two outputs then gave the signals $\Delta R/\Delta\lambda$ and R (or $\Delta R/R\Delta\lambda$ and $1/R$).

Maximum slit width and modulation amplitude were chosen with precaution such that lineshapes of the fine structures in the derivative spectrum were not distorted. The sharpest structure in our spectra had a width larger than 60 Å. The derivative spectrum $\Delta R(\lambda)/R\Delta\lambda$ vs λ was recorded by a chart recorder. A simple computer program was then used to convert the spectrum to $\Delta R(E)/R\Delta E$ vs the energy E in eV. The conversion makes the structures at higher frequencies less pronounced, but the corresponding noise amplitude also decreases proportionally.

Therefore, small wiggles in the uv region of our spectra $\Delta R/R\Delta E$ vs E deserve full attention as true structures.

In order to make sure that the observed structures of the spectrum were characteristics of the sample rather than other spurious effects, we used the spectrum of aluminum as a reference. Aluminum was chosen because its spectrum shows little structure in the region in which we were interested.

B. The Dewar

The optical dewar was manufactured by Janis Research Company. Temperature of the sample can be varied continuously from the liquid He temperature to the room temperature. The temperature control has a long-term stability of better than 1°K/hr . A copper-constantan thermocouple was used to measure the temperature over the whole range of interest with an accuracy of $\pm 1^\circ\text{K}$. This was sufficient for our purpose since the spectrum changes gradually with temperature. Most of our spectra were taken at 5°K , 80°K , and 300°K .

C. The Samples. All the samples we measured were wafers of single crystals with (1,1,1) orientation. The samples were polished and etched following the standard procedure.¹³ For good reproducibility, a crystal surface free of mechanical distortion and chemical contamination was essential.³ Surface contamination often produced more distortion of the spectrum in the uv than in the visible. All our measurements were made on freshly prepared samples.

The samples were of either n- or p- type, doped with a carrier

concentration in the range between 10^{13} and 10^{17} cm^{-3} . We would expect that the wavelength modulation spectrum is independent of the carrier concentration. This was confirmed by measurements on two samples of Si with carrier concentrations of 10^{13} and 10^{17} cm^{-3} respectively.

III. EXPERIMENTAL RESULTS

In Fig. 1, we show a derivative spectrum, $\Delta R(E)/R\Delta E$, of InSb at 5°K , together with the normal reflectivity spectrum $R(E)$. That the derivative spectrum has a better resolution is clearly shown. Differentiation of $R(E)$ on a computer yields the same derivative spectrum, but with a much smaller signal-to-noise ratio.

In Figs. 2-7, we present the derivative spectra, $\Delta R(E)/R\Delta E$ of GaAs, GaSb, InAs, InSb, Ge, and Si respectively at three different temperatures, 5°K , 80°K , and 300°K . Compared with the derivative spectra obtained from electroreflectance³ and thermorelectance⁷ measurements, our spectra give the same gross features, but show definite improvement with more fine structures, especially at low temperatures. As an example, we reproduce in Fig. 8 the electroreflectance and the thermorelectance spectra of InAs obtained by Cardona, et al.^{3,7} The temperature variation of the wavelength-modulation spectra is fairly striking, although the change is rather gradual. All the main structures shifted to higher energies when the temperature is lowered. The structures generally become sharper at lower temperatures.

The spectra of the six crystals are very much alike, reflecting the similarity of their band structures. Following partially the notations of Cardona, et al.,² we divide the structures in each spectrum

into groups, labelled by E_0 , E_1 , E'_0 , E_2 , E'_1 , etc., as shown in the figures. Similar groups (having the same label) in different semiconductors are believed to come from transitions in the similar general areas of the band structures. The group E_0 , corresponding to transitions near the direct fundamental energy gap, has not been covered by our experiments.

As shown in Figs. 2-7, each group may contain many structures. These structures presumably come from several reflectivity peaks superimposed on top of one another. Decomposition of a composite line into individual peaks is always somewhat arbitrary. In our case, the decomposition was made with the following general rules:

- (1) The low-temperature spectrum of a composite line should be decomposed into a minimum number of individual lines with simple lineshapes.
- (2) Recomposition of these individual lines with broadened linewidths should yield the high-temperature spectrum of the composite line.
- (3) Similarity in the spectra of different semiconductors should be used as a guide line in the decomposition.

With these rules, we found little ambiguity in decomposing our spectra although the positions of the components may not be very accurate and their shapes somewhat arbitrary. An example of the decomposition is shown in Fig. 9. In Table I, we list the positions of all the reflectivity peaks obtained from decomposition of our spectra at 5°K for the six semiconductors. The accuracy of the most uncertain values in the Table

is estimated to be better than ± 0.03 eV.

We now proceed to comment briefly on the low-temperature spectrum of each semiconductor separately.

GaAs (Fig. 2). Although the spectrum below 2.7 eV is not shown in Fig. 2, we have explored this region carefully. We have not been able to find the small structures at 2.3 and 2.6 eV observed by Greenway.¹⁴ In the E_1 region, our spectrum confirms the absence of the small structures suggested by Lukes, et al.¹⁵ Decomposition of the spectrum in the E_0' region yields two reflectivity peaks. Decomposition in the E_2 region is somewhat arbitrary. To be consistent with the spectra of other III-V compounds, we should decompose the E_2 group into a strong broad peak with three small peaks at higher energies. Part of the E_2 spectrum above 6 eV was cut off by our spectrometer.

GaSb (Fig. 3). The structure at 1.9 eV observed by Greenway¹⁴ is absent in our spectrum. Decomposition of the spectrum gives unambiguously two peaks in the E_0' region, one strong and three weak in the E_2 region, and two in the E_1' region. The shape of the spectrum near 6 eV indicates the presence of additional structures just above 6 eV belonging to the E_1' group.

InAs (Fig. 4). We cannot identify in our spectrum the peaks at 2.2 and 2.45 eV suggested by Greenway.¹⁴ The spectrum of InAs is somewhat different from those of other III-V compounds in the sense that the E_0' and the E_2 regions overlap. We can unambiguously decompose the structures in this $E_0' + E_2$ region into six reflectivity peaks. We assign the two weak ones at lower frequencies to the E_0' group and

the rest to the E_2 group. Note that the spectrum of InAs appear to have a very strong temperature dependence.

InSb (Fig. 5). The spectrum of InSb looks very much similar to that of GaSb. Decomposition of the spectrum gives two peaks in the E_0' region, four in the E_2 region, and three in the E_1 region.

Ge (Fig. 6). The spectrum of Ge is still quite similar to those of III-V compounds, but with less structures. Decomposition of the spectrum yields one peak in the E_0' region, one strong and one weak in the E_2 region, and two in the E_1' region.

Si (Fig. 7). Because of the difference in the band structures near the direct gap, the spectrum of Si is somewhat different from those of others in the E_1 and E_0' regions. Here, the E_1 peak appears at higher energy and overlaps with the E_0' peak. We assign the peak at 3.4 eV to E_0' , and the one at 3.45 eV to E_1 . The spectrum in the E_2 and E_1 regions are similar to those of others. We can decompose the spectrum into one strong and one weak peaks in the E_2 region, and one in the E_1' region.

IV. DISCUSSION

A qualitative comparison between our spectra and the spectra obtained from electroreflectance^{2,3} and thermorelectance^{6,7} measurements should be made. At room temperature, our spectra compare well with thermorelectance spectra. The electroreflectance spectra generally show more structures, but the assignment of reflectivity peaks is somewhat arbitrary. Our low-temperature spectra appear better resolved than either thermorelectance or electroreflectance spectra. While we

recognize no new structure in the E_1 region, there are generally more distinct structures in E'_0 , E_2 , and E'_1 regions.

We must now identify the various reflectivity peaks in our spectra with particular interband transitions in the crystals. It was believed that a reflectivity peak which is usually originated from an absorption peak was likely to come from critical interband transitions at a point of high symmetry. Recent calculations,^{1,16} however, indicate that a strong reflectivity peak should come from critical interband transitions over a region in the Brillouin zone, not necessarily around a point of high symmetry. We shall use this as a general principle in the assignment of reflectivity peaks.

For the purpose of illustration, we reproduce in Fig. 10 the band structure of GaSb.^{1,17} The band structures of the other semiconductors, except Si, are qualitatively similar to that of GaSb. For Si, the point Γ_1 (Γ'_2) appears to be higher in energy than Γ_{15} . (We use here the zincblende group notations for Si and Ge.) The band structure of Fig. 10 should be modified accordingly.¹⁸ A direct consequence is that Si has an indirect energy gap along Δ . In Fig. 10, we use arrows to indicate critical transitions with large joint densities of states in those general areas of the Brillouin zone. These are the transitions which may give rise to the observed reflectivity peaks.

Let us now discuss each spectral region separately for the six crystals. Assignment of all the observed reflectivity peaks to the corresponding interband transitions is summarized in Table I. Our assignment is based on the available information about the band structures of these semiconductors.^{1,16-23} Unless specified, we shall

always refer to the spectra at 5°K.

A. The E_1 Region

Except for Si, all our spectra show a sharp doublet. It is generally agreed that this doublet corresponds to $\Lambda_3 \rightarrow \Lambda_1$ transitions with the Λ_3 level spin-orbit splitted.^{1,3} A simple analysis²³ shows that the spin-orbit splitting of Λ_3 near L should be around 2/3 of the spin-orbit splitting at Γ_{15} . No spin-orbit splitting should exist for the Λ_1 level.²⁴ As shown in Table II, the observed splitting of the doublet confirms the above 2/3 rule.

The existence of reflectivity peaks for $L_3 \rightarrow L_1$ transitions has been a mystery.^{1,14} The fact that we have seen no additional structure in the E_1 region indicates that either the $L_3 \rightarrow L_1$ transitions are too weak or they are hidden in the $\Lambda_3 \rightarrow \Lambda_1$ structure.

The band structure of Si puts $\Gamma_1(\Gamma'_2)$ above Γ_{15} . This makes the $\Lambda_3 \rightarrow \Lambda_1$ transitions and the $\Delta_5 \rightarrow \Delta_1(4-5)$ transitions partially degenerate in energy.¹⁸ As shown in Fig. 7, there are two overlapping reflectivity peaks at 3.40 and 3.45 eV. Assuming that similar transitions in different crystals would yield reflectivity peaks of similar strength, we should assign the 3.45 eV peak to the $\Lambda_3 \rightarrow \Lambda_1$ transitions, and the 3.40 eV peak to the $\Delta_5 \rightarrow \Delta_1(4-5)$ transitions. The spin-orbit coupling in Si is small. It gives a splitting of 0.04 eV at $\Gamma_{15}(\Gamma'_{25})$,^{3,25} and even smaller splittings along Λ_3 and Δ_5 .²³ The resolution of our Si spectrum is clearly not sufficient to show the spin-orbit splitting of either $\Lambda_3 \rightarrow \Lambda_1$ or $\Delta_5 \rightarrow \Delta_1(4-5)$ transitions. We therefore rule out the possibility that the two peaks at 3.40 and 3.45 eV could correspond to the spin-orbit doublet of the $\Lambda_3 \rightarrow \Lambda_1$ transitions.

Figures 2-7 show that all the E_1 peaks appear significantly sharper at lower temperatures. This suggests possible exciton effect associated with the $\Lambda_3 \rightarrow \Lambda_1$ transitions. Shaklee, et al⁹ have shown that the existence of hyperbolic excitons at Λ can explain the observed lineshape of the E_1 peaks. Rowe, et al¹¹ have also confirmed the existence of hyperbolic excitons from the pressure dependence of the E_1 peaks. Our spectra suggest that this exciton effect is present in all III-V and group IV semiconductors.

B. The E'_0 Region

We can identify a doublet in the E'_0 group for the four III-IV compounds and a single peak for the two group-IV elements. These E'_0 peaks were originally assigned to 4-5 transitions at or near Γ ,^{14,3} but the low joint density of states near Γ rules out such an assignment.^{17,19} The peaks are more likely due to $\Delta_5 \rightarrow \Delta_1$ (4-5) transitions away from Γ .^{17,19} Only the Δ_5 level is spin-orbit splitted. Pseudopotential^{17,25} and $\mathbf{k} \cdot \mathbf{p}$ calculations²¹ indicate that the spin-orbit splitting along Δ_5 should be even smaller than the splitting at L_3 (band 4) (which is 2/3 of the splitting at Γ_{15}). Our results agree well with this assertion. The observed E'_0 doublet for a III-V compound has indeed a splitting smaller than that of the E_1 doublet (see Table II). In Ge, the symmetry points at X_5 become degenerate, and calculation shows that the spin-orbit splitting along $\Delta_5(4)$ should be small.²³ We would not expect to resolve the spin-orbit doublet in the Ge spectrum. We should therefore assign the single E'_0 peak of Ge to $\Delta_5 \rightarrow \Delta_1$ (4-5) transitions. The same is true for Si, which has even smaller spin-orbit coupling.

C. The E_2 Region

Our spectra for all the six crystals seem rather complicated in this region. They generally show more structures than either electroreflectance or thermorefectance spectra. However, we can always decompose the E_2 group quite unambiguously into a broad strong reflectivity peak and several small peaks at higher energies. Pseudopotential calculation^{1,16,17,19} indicates that this broad peak should be due to $\Sigma_2 \rightarrow \Sigma_1$ (4 \rightarrow 5) transitions over a large region in the Brillouin zone. The spin-orbit splitting along Σ_1 is small,^{17,23} and would be difficult to resolve. From the band structure of Fig. 10, one might expect to observe a reflectivity peak corresponding to $X_5 \rightarrow X_1$ transitions at an energy between $\Sigma_2 \rightarrow \Sigma_1$ (4-5) and $\Delta_5 \rightarrow \Delta_1$ (4-5) transitions. We cannot recognize any such structure in all our spectra. This suggests that either $X_5 \rightarrow X_1$ transitions are too weak or they are hidden in the broad $\Sigma_2 \rightarrow \Sigma_1$ (4-5) peak.

The small E_2 peaks have higher energies than the $\Sigma_2 \rightarrow \Sigma_1$ (4-5) transitions. As seen from Fig. 10, they should correspond to transitions between the valence band (band 4) and the second conduction band (band 6). There is some ambiguity in decomposing the small E_2 structures, but we can unambiguously identify one peak in Ge, and Si, three in InAs, InSb, and GaSb, and probably also three in GaAs. We then recognize that for all the III-V compounds, the spacing between two of the three peaks agrees quite well with the spin-orbit splitting of the Δ_5 level (see Table I). We therefore assign the doublet to 4-6 transitions along Δ (close to X).²⁶ The same transitions should give rise to only one reflectivity peak in Ge and Si, since the spin-orbit splitting along

Δ_5 for these two elements is small.^{23,25} Accordingly, the small E_2 peak of Ge and Si should correspond to $\Delta_5 \rightarrow \Delta_1$ (4-6) transitions. The remaining small E_2 peak of the III-V compounds is assigned to 4-6 transitions around Σ as suggested by pseudopotential calculation.²⁷ Such a peak did not show up in the spectra of Ge and Si presumably because of the slight difference in their band structures.

D. The E_1 Region. Our spectra, limited by the uv cutoff of the spectrometer, cover only part of the E_1 region in Si, Ge, GaSb, and InSb, and none in GaAs and InAs. The E_1 peaks are normally assigned to 4-6 transitions along Λ close to L.^{3,28} Both Λ_3 levels are spin-orbit splitted, but the splitting of $\Lambda_3(6)$ is expected to be considerably smaller than that of $\Lambda_3(4)$.^{17,20} We should therefore expect to see two doublets separated by the spin-orbit splitting of $\Lambda_3(4)$.

In Si, the spin-orbit coupling is small, and we have observed only one unresolved reflectivity peak as expected. In Ge, we can identify two peaks with a separation somewhat larger than the splitting of the $\Lambda_3 \rightarrow \Lambda_1$ doublet. This suggests that the splitting of $\Lambda_3(6)$ in Ge is very small, and the observed $\Lambda_3 \rightarrow \Lambda_3$ transitions are closer to L than the $\Lambda_3 \rightarrow \Lambda_1$ transitions. In InSb, where the spin-orbit coupling is larger, we have actually observed three peaks with the fourth one being cut off by our spectrometer. The spin-orbit splitting of $\Lambda_3(4)$ derived from them is again somewhat larger than the splitting of the $\Lambda_3 \rightarrow \Lambda_1$ doublet. The separation of the two closely overlapping peaks gives the spin-orbit splitting of $\Lambda_3(6)$ near L (see Table II). In GaSb, we can observe only one doublet with a small splitting corresponding to the splitting of $\Lambda_3(6)$. The other doublet at higher energy should be

outside the range of our spectrometer.

From the above description, we have seen that the consistency of our assignment of reflectivity peaks is remarkable good. For more quantitative discussion, one must, however, resort to pseudopotential calculations.¹ We have deduced from our spectra the spin-orbit splittings at various symmetry points in different crystals. The results are summarized in Table II.

We can also obtain from our spectra at various temperatures some information about the temperature dependence of the band structures. Figures 2-7 show that all the major reflectivity peaks shift to lower energies at higher temperatures. This temperature effect can be understood qualitatively from thermal expansion of crystal lattices and the Debye-Waller effect.²⁹ Expansion of a lattice should reduce the energy separation between bands. Lattice vibration at finite temperatures should decrease the effective core potential by the Debye-Waller factor, and hence decrease the splittings between bands.²⁹

The temperature shift of a reflectivity peak is rather smooth and gradual. We have studied the temperature effect on GaAs in more detail. Figure 11 shows the temperature shifts of the E_1 doublet and the major E_2 peak of GaAs. The three curves behave similarly. We can deduce from these curves an average temperature coefficient of $dE/dT = (5.3 \pm 0.4) \times 10^{-4}$ eV/ $^{\circ}$ K for the E_1 doublet and $(3.6 \pm 0.4) \times 10^{-4}$ eV/ $^{\circ}$ K for the E_2 peak in the temperature range between 80 and 300 $^{\circ}$ K. The observed temperature shifts also fit well with the exponential dependence

$$\Delta E(T) \equiv E(T) - E(5^\circ\text{K}) = A \exp(-B/T)$$

with, for example, $A = 0.28$ eV, $B = 320^\circ\text{K}$ for the E_2 peak. In the other crystals, we have observed similar temperature dependence of the reflectivity peaks. We present in Table III the observed temperature coefficients of the E_1 and the major E_2 peaks for all the six crystals. Note that Si has a smaller temperature dependence than the other crystals, presumably because it has a higher Debye temperature.

As seen from our spectra, all the structures become sharper at lower temperatures. This is presumably due to reduction of lifetime broadening. In particular, the E_1 peaks have been associated with hyperbolic excitons partly for this reason. There are also remarkable sharpening of E_2 and E_1 peaks at low temperatures. It would be interesting to know whether exciton effects are also important in these transitions.

V. CONCLUSION

We have demonstrated in this paper the superiority of wavelength modulation spectroscopy. Our derivative spectra of the six semiconductors show clear improvement on the spectral resolution over other techniques. In particular, our low-temperature spectra give more clearly-defined reflectivity peaks than either electroreflectance or thermoreflectance spectra. With available information about the band structures, the spin-orbit splittings, and similarities among the semiconductors, we can consistently assign all the observed reflectivity peaks to proper critical transitions between bands. Values of spin-orbit splittings at various symmetry points can then be deduced. Results agree well with simple theoretical estimates.

Our measurements at various temperatures also yield valuable

information about the temperature dependence of the band structures. As predicted by qualitative argument, all the reflectivity peaks shift to higher energies at lower temperatures. The structures in the spectra generally become much more pronounced at lower temperatures. Sharpening of the E_1 peaks at low temperatures is particularly striking and can be explained in terms of reduction of lifetime broadening of the hyperbolic excitons associated with Λ . Whether the exciton effect is also important in the other transitions remains to be investigated.

To help us make sure that our assignment of reflectivity peaks is correct, measurements on samples under uniaxial stress should be performed. That a stress can be exerted on the sample without much complication is another advantage of the wavelength-modulation scheme. The pressure dependence of the reflectivity spectrum should also yield valuable information about hyperbolic excitons associated at various symmetry points.³⁰

ACKNOWLEDGEMENTS

We would like to thank M. L. Cohen, J. P. Walter, R. Cahn, and C. Y. Fong for many helpful discussions, and M. P. Klein for technical help.

This work was done under the auspices of the United States Atomic Energy Commission.

REFERENCES

1. M. L. Cohen and V. Heine, The Fitting of Pseudopotentials to Experimental Data and Their Subsequent Applications (to be published in Solid State Physics, edited by F. Seitz, D. Turnbull, and H. Ehrenreich, Academic Press, Inc., New York); and references therein.
2. B. O. Saraphin and N. Bottka, Phys. Rev. 145, 628 (1966).
3. M. Cardona, K. Shaklee, and F. H. Pollak, Phys. Rev. 154, 696 (1967).
4. W. E. Engler, H. Fritsche, M. Garfinkel, and J. J. Tiemann, Phys. Rev. Letters 14, 1069 (1965);
M. Garfinkel, J. J. Tiemann, and W. E. Engler, Phys. Rev. 148, 695 (1966).
5. G. W. Gobeli and E. O. Kane, Phys. Rev. Letters 15, 142 (1965).
6. B. Batz, Solid State Commun. 4, 241 (1966).
7. M. Matatagui, A. G. Thompson, and M. Cardona, Phys. Rev. 176, 950 (1968).
8. See, for example, I. Baslev, Phys. Rev. 143, 676 (1966).
9. K. L. Shaklee, J. E. Rowe, and M. Cardona, Phys. Rev. 174, 828 (1968).
10. J. E. Rowe, M. Cardona, and K. L. Shaklee, Solid State Commun. 7, 441 (1969).
11. J. E. Rowe, F. H. Pollak, and M. Cardona, Phys. Rev. Letters 22, 933 (1969).
12. Ricardo R. L. Zucca and Y. R. Shen (to be published).
13. H. C. Gatos and M. C. Levine, Progress in Semiconductors, edited by A. F. Gibson and R. E. Burgess (Temple Press, London, 1965 Vol. 9, p. 1.
14. D. L. Greenway, Phys. Rev. Letters 9, 97 (1962);
D. L. Greenway and M. Cardona, Proceedings of the International Conference on The Physics of Semiconductors, Exeter, 1962, p. 666.

15. F. Lukes and E. Schmidt, Proceedings of the International Conference on The Physics of Semiconductors, Exeter, 1962, p. 389.
16. E. O. Kane, Phys. Rev. 146, 558 (1966).
17. R. Cahn and M. L. Cohen, (to be published).
18. M. L. Cohen and T. K. Bergstresser, Phys. Rev. 141, 789 (1966).
19. J. P. Walter and M. L. Cohen (to be published).
20. H. I. Zhang and J. Callaway, Phys. Rev. 181, 1163 (1969).
21. F. H. Pollak, C. W. Higginbotham, and M. Cardona, J. Phys. Soc. (Japan) 21, Supplement, p. 20 (1966).
22. F. Herman, R. L. Kortum, C. D. Kuglin, J. P. Van Dyke, and S. Skillman, Methods of Computational Physics, edited by B. Alder, S. Fernbach, and M. Rotenberg (Academic Press, Inc., New York, 1968) V. 8, p. 193.
23. L. R. Savaria and D. Brust, Phys. Rev. 176, 915 (1968).
24. R. H. Parmenter, Phys. Rev. 100, 573 (1955).
25. F. Herman, C. K. Kuglin, K. F. Cuff, and R. L. Kortum, Phys. Rev. Letters 11, 541 (1963).
26. This assignment is also suggested by pseudopotential calculation for GaSb which shows two spin-orbit splitted peaks coming from 4-6 transitions along Δ in the neighborhood of X. See Ref. 17.
27. J. P. Walter, Private communications.
28. M. Cardona, Proceedings of the 7th International Conference on the Physics of Semiconductors, Paris, 1964 (Dumond, Paris, 1964) p. 181.
29. J. P. Walter, R. R. L. Zucca, M. L. Cohen, and Y. R. Shen (to be published).
30. E. O. Kane, Phys. Rev. 178, 1368 (1969).

TABLE CAPTIONS

Table I. Energies (eV) of observed reflectivity peaks in the six crystals. Assignment of various peaks to particular interband transitions is also given.

Table II. Spin-orbit splittings (in eV) at various points in the band structures of the six crystals, obtained from analysis of our reflectivity spectra. The values of spin-orbit splittings at Γ_{15} are obtained from the reference K. L. Shaklee, J. E. Rowe, and M. Cardona, Phys. Rev. 174, 828 (1968).

Table III. Average temperature shifts in unit of 10^{-4} eV/ $^{\circ}$ K between 80 and 300 $^{\circ}$ K for the E_1 doublet and the major E_2 peak in the six crystals. Accuracy is $\pm 0.4 \times 10^{-4}$ eV/ $^{\circ}$ K.

FIGURE CAPTIONS

- Fig. 1. Reflectivity spectrum and logarithmic derivative reflectivity spectrum of InSb at 5°K in the range between 1.75 and 6 eV.
- Fig. 2. Logarithmic derivative of the reflectivity spectrum of GaAs at 5, 80, and 300°K.
- Fig. 3. Logarithmic derivative of the reflectivity spectrum of GaSb at 5, 80, and 300°K.
- Fig. 4. Logarithmic derivative of the reflectivity spectrum of InAs at 5, 80, and 300°K.
- Fig. 5. Logarithmic derivative of the reflectivity spectrum of InSb at 5, 80, and 300°K.
- Fig. 6. Logarithmic derivative of the reflectivity spectrum of Ge at 5, 80, and 300°K.
- Fig. 7. Logarithmic derivative of the reflectivity spectrum of Si at 5, 80, and 300°K.
- Fig. 8(a). Electroreflectance spectrum of InAs at room temperature (reproduced from Ref. 3).
- (b). Thermoreflectance spectrum of InAs at 77°K (reproduced from Ref. 7).
- Fig. 9. Decomposition of the derivative reflectivity spectrum of InSb at 5°K into many components according to the general rules stated in the text.
- Fig. 10. Band structure of GaSb (reproduced from Ref. 1). Arrows indicate interband transitions which are possibly responsible for the observed reflectivity peaks.
- Fig. 11. Temperature shifts of the E_1 doublet and the major E_2 reflectivity peak of GaAs.

	E_1		E_0		E_2				E_1	
	$\Delta_3 \rightarrow \Lambda_3$		$\Delta_5 \rightarrow \Delta_1 (4 \rightarrow 5)$		$\Sigma_2 \rightarrow \Sigma_1 (4 \rightarrow 5)$	$\Sigma_2 \rightarrow \Sigma_1 (4 \rightarrow 6)$	$\Delta_5 \rightarrow \Delta_1 (4 \rightarrow 6)$		$\Lambda_3 \rightarrow \Lambda_3$	
GaAs	3.017	3.245	4.44	4.60	5.11	5.64	5.91	6.07 (?)		
GaSb	2.154	2.596	3.35	3.69	4.35	4.55	4.75	5.07	5.51	5.65
InAs	2.612	2.879	4.39	4.58	4.74	4.85	5.33	5.52		
InSb	1.983	2.478	3.39	3.78	4.23	4.75	4.56	4.92	5.33	5.50 5.96
Ge	2.222	2.420		3.20	4.49			5.01		5.65 5.88
Si		3.45		3.40	4.44			5.60		5.53
Estimated Uncertainty	± 0.004		± 0.008		± 0.01	± 0.03	± 0.03		± 0.03	

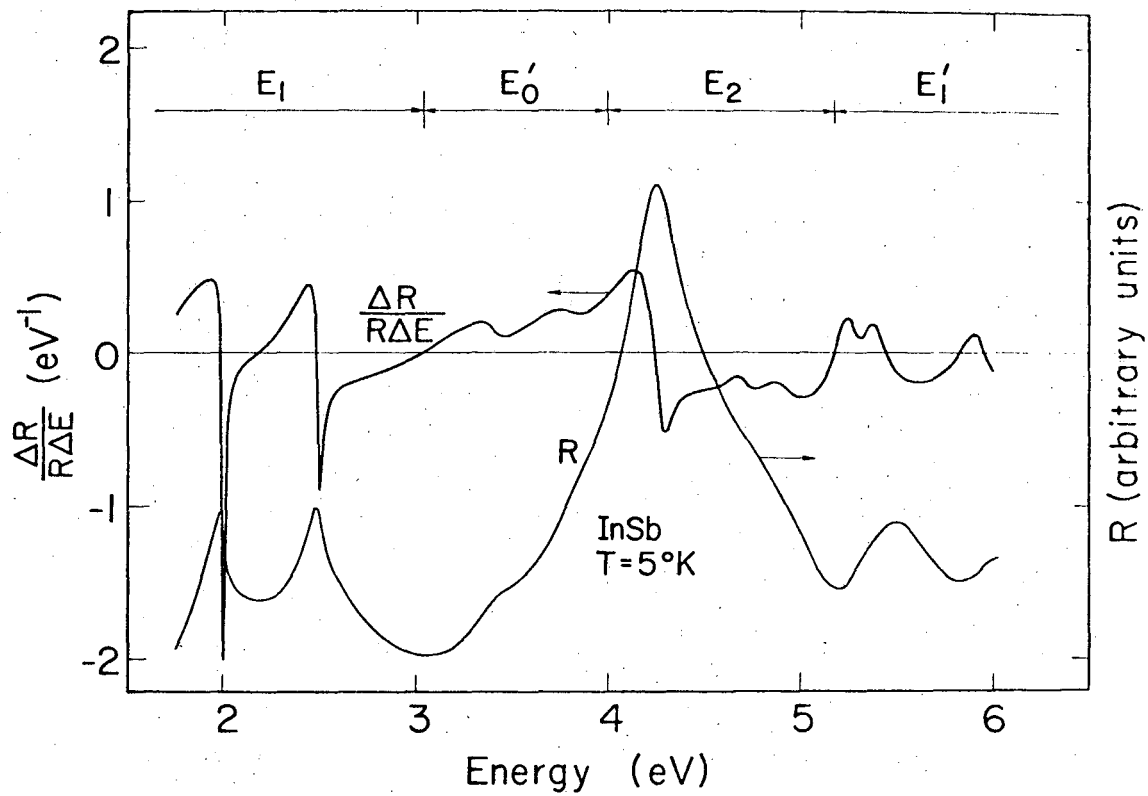
TABLE I

5-0 splitting at Material	Γ_{15}	$\Delta_3(4)$		$\Lambda_3(6)$	Δ_5	
		from $\Lambda_3 \rightarrow \Lambda_1$ transitions	from $\Delta_3 \rightarrow \Lambda_3$ transitions	from $\Lambda_3 \rightarrow \Lambda_3$ transitions	from $\Delta_5 \rightarrow \Delta_1$ (4→5) transitions	from $\Delta_5 \rightarrow \Delta_1$ (4→6) transitions
GaAs	0.34	0.22		0.14	0.16	0.16(estimate)
GaSb	0.80	0.45			0.34	0.32
InAs	0.43	0.27		0.17	0.19	0.19
InSb	0.82	0.50	0.63		0.39	0.36
Ge	0.29	0.20	0.23			
Si	0.04					

TABLE II

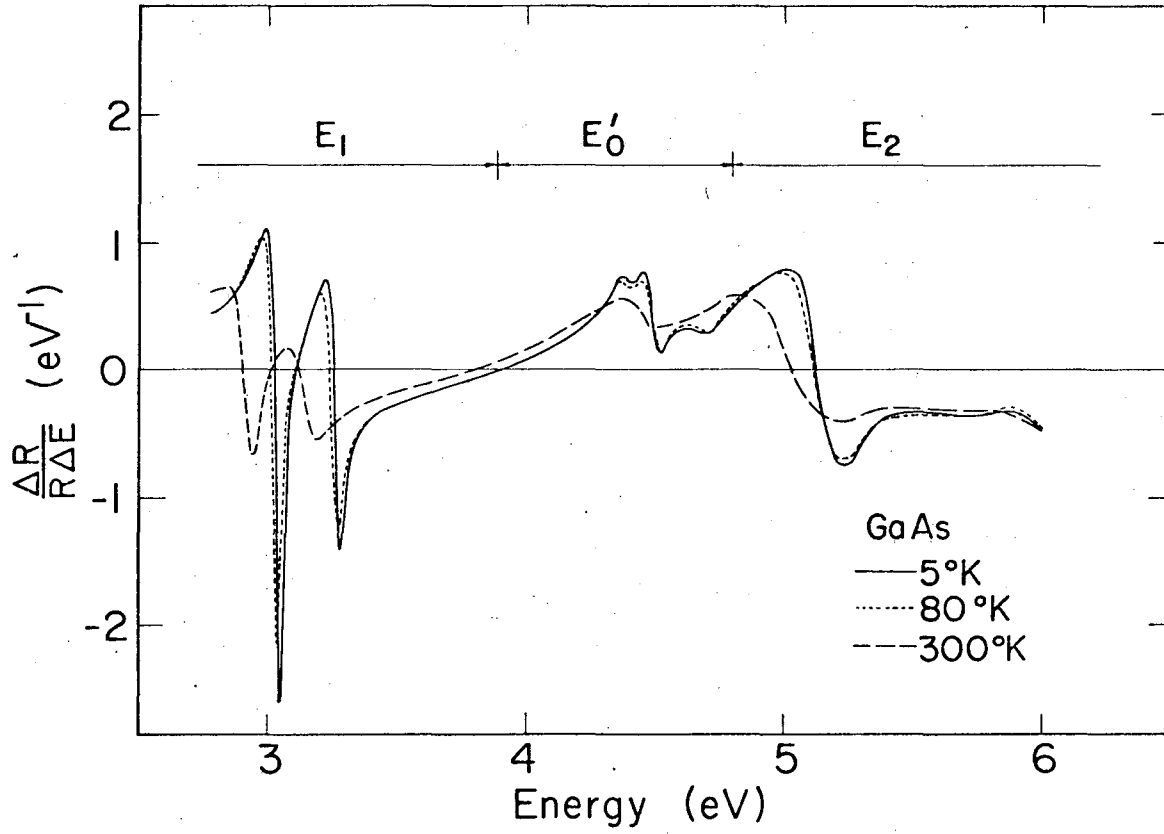
	GaAs	GaSb	InAs	InSb	Ge	Si
E_1	-5.3	-4.5	-5.0	-4.4	-4.2	-2.2
E_2	-3.6	-4.1	-5.6	-3.6	-2.4	-2.2

TABLE III



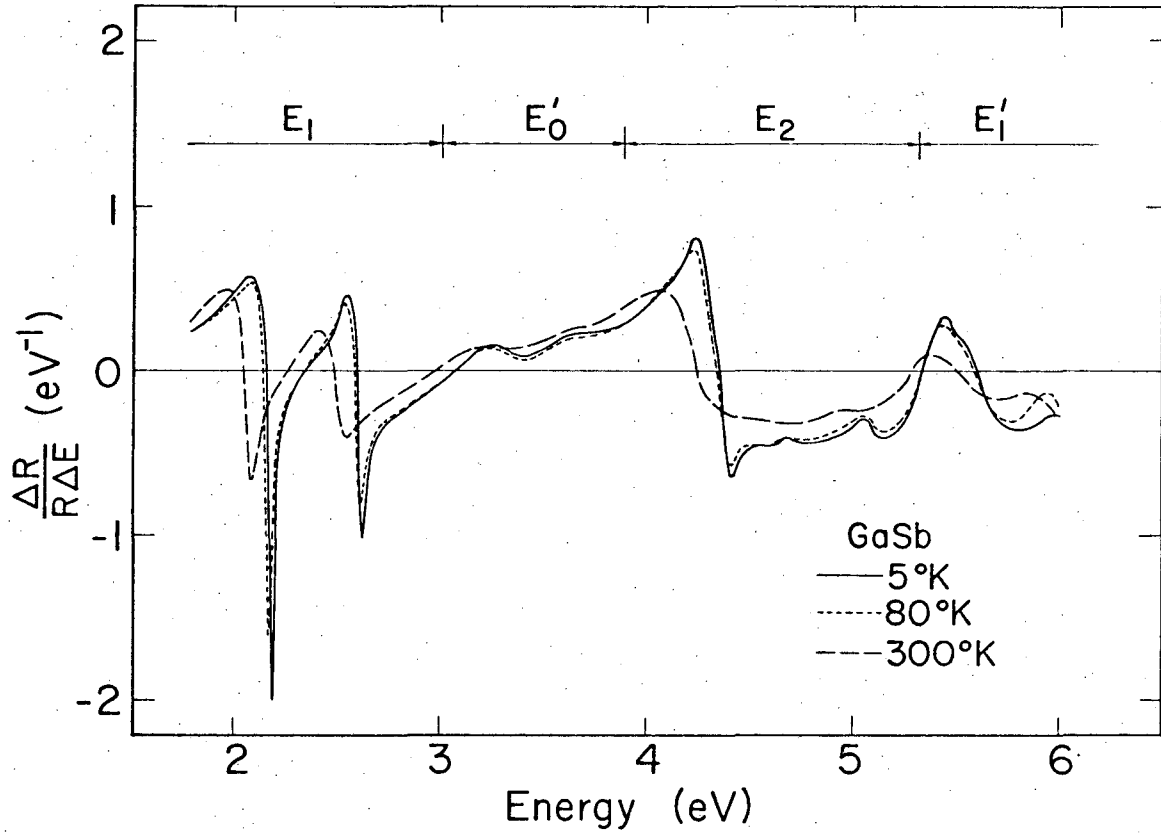
XBL699-3865

Fig. 1



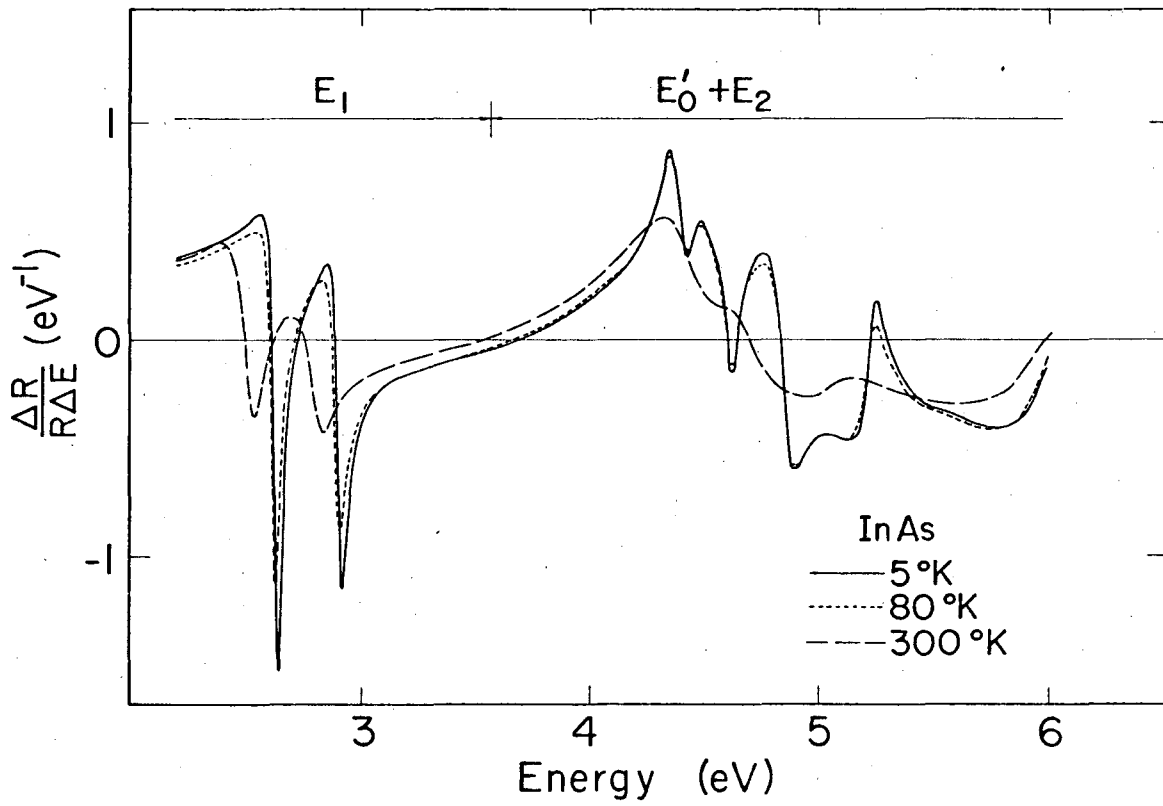
XBL699-3866

Fig. 2



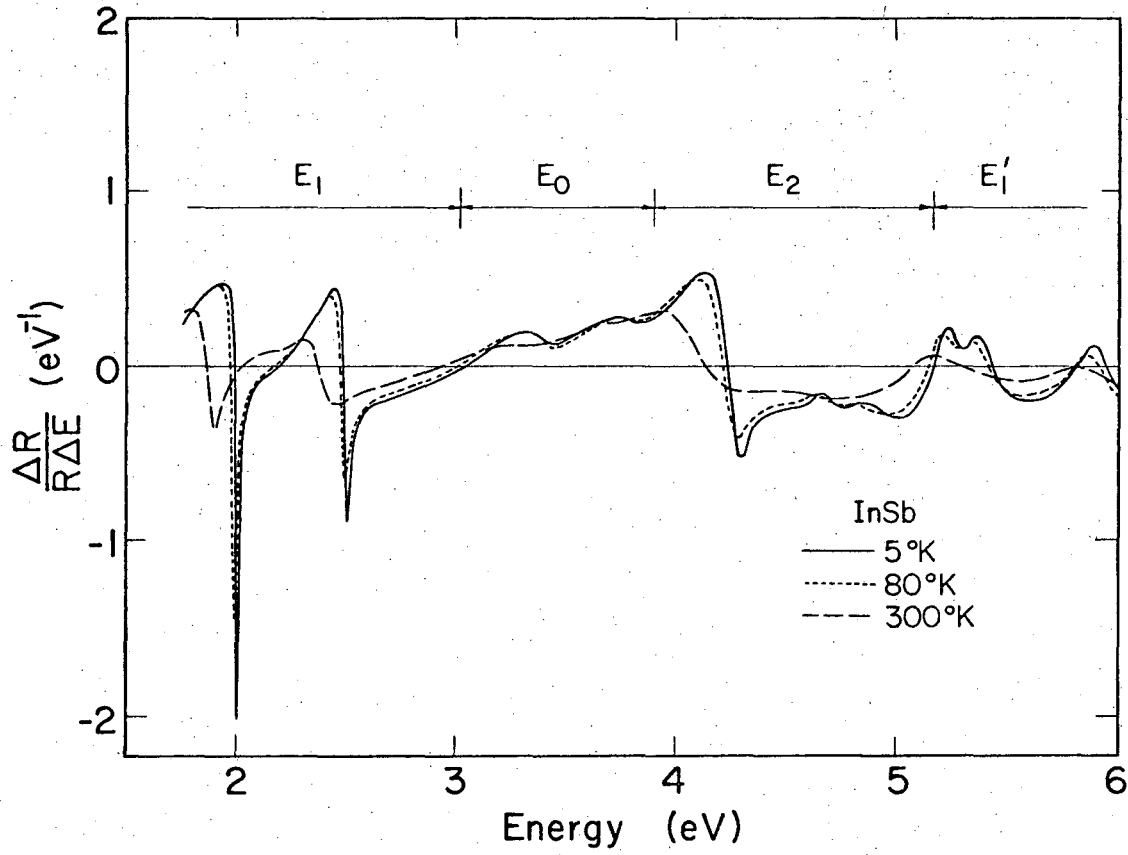
XBL699-3867

Fig. 3



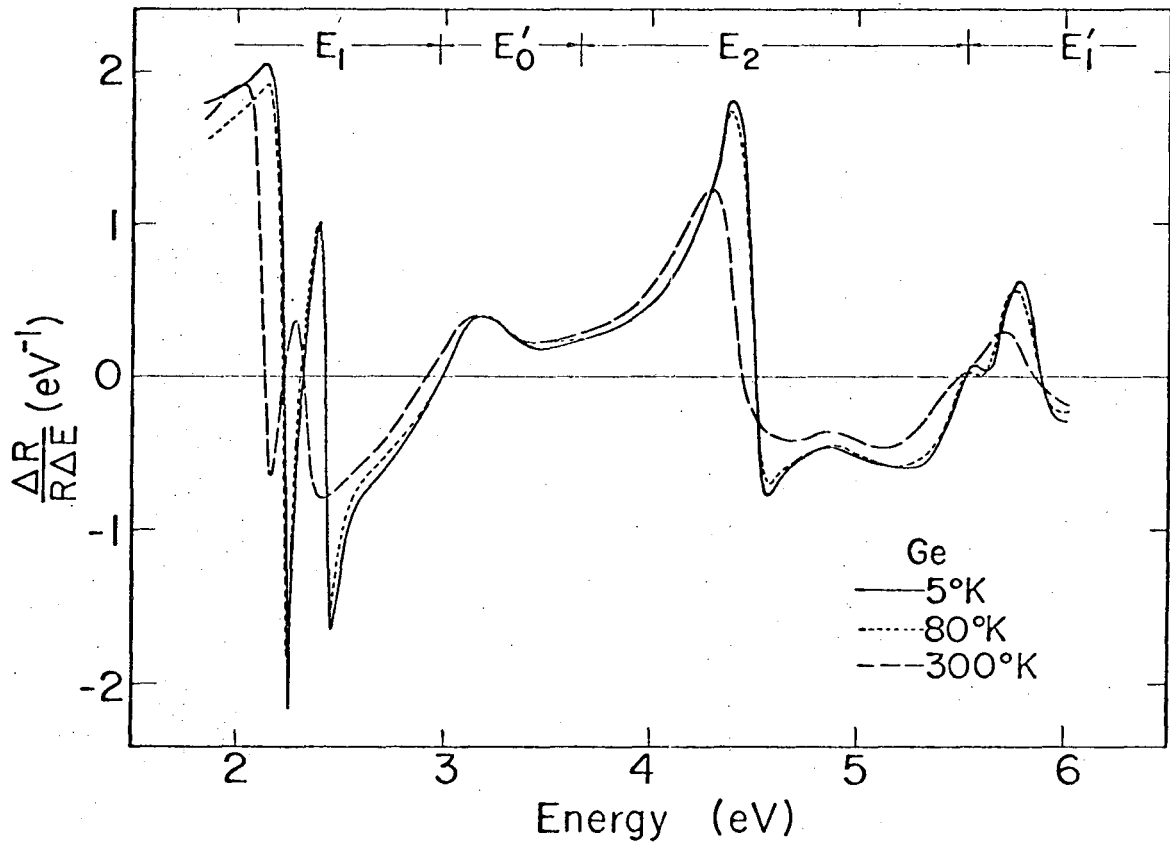
XBL699-3868

Fig. 4



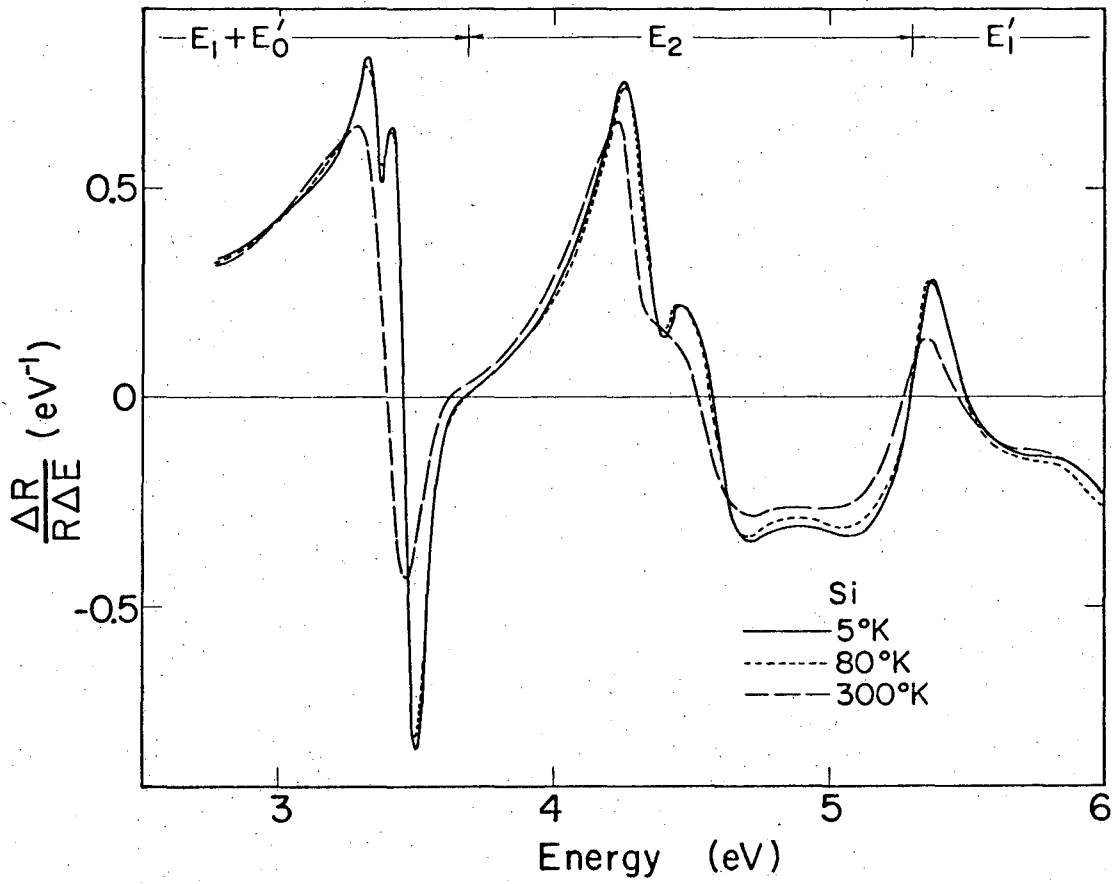
XBL699-3869

Fig. 5



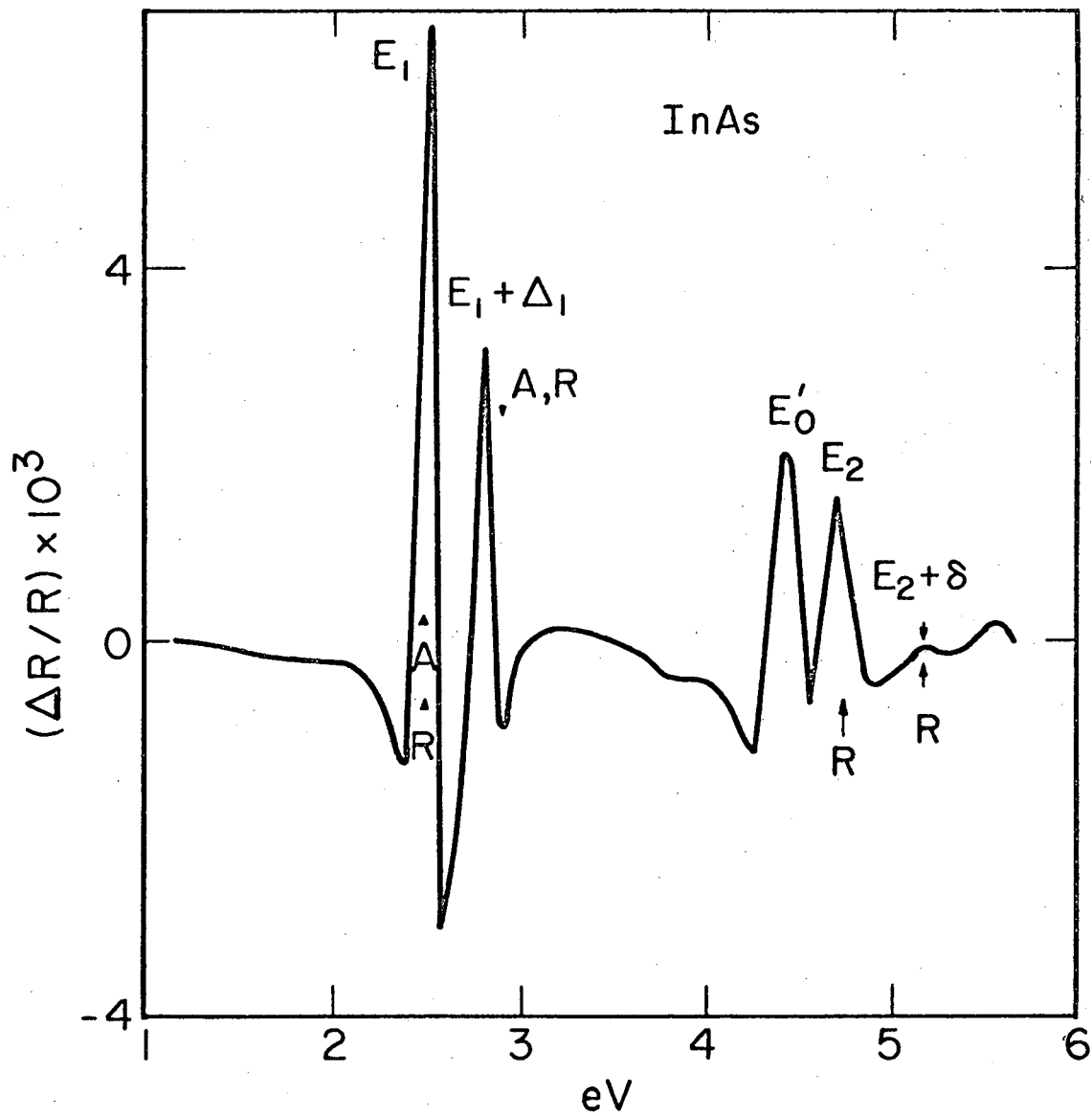
XBL699-3870

Fig. 6



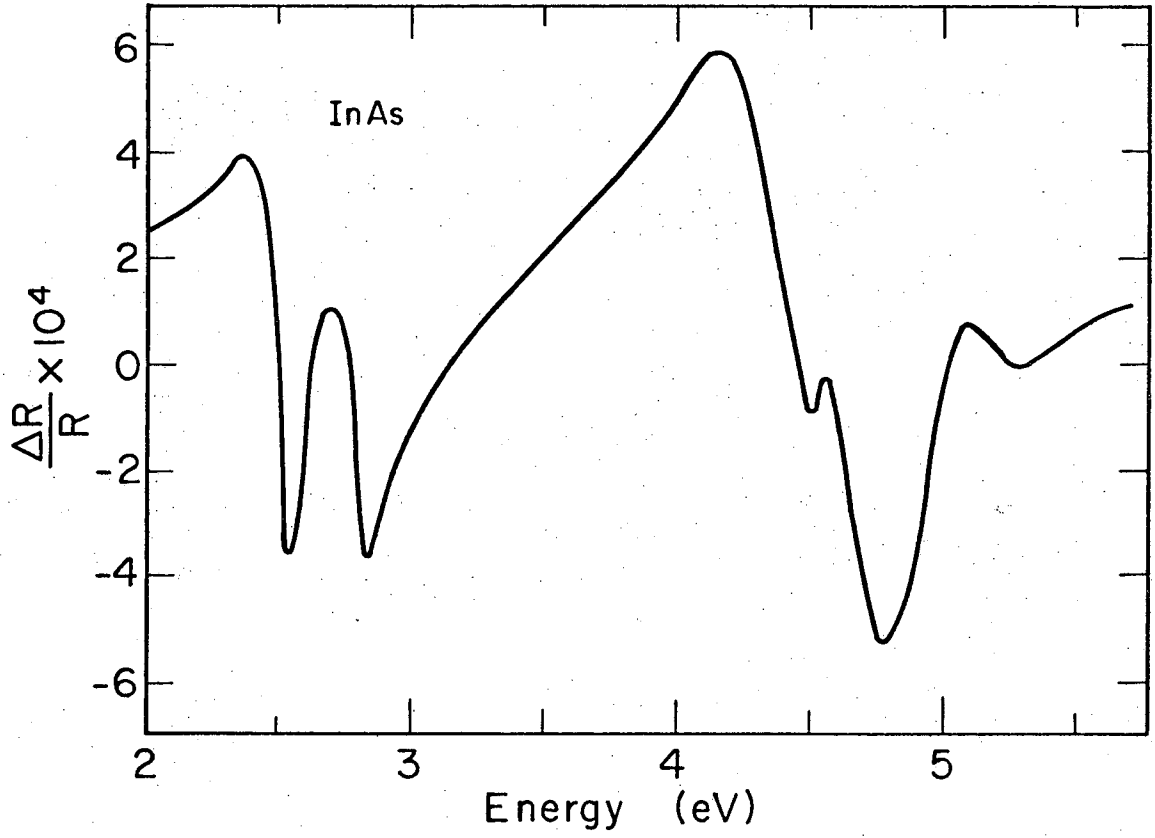
XBL699-3871

Fig. 7



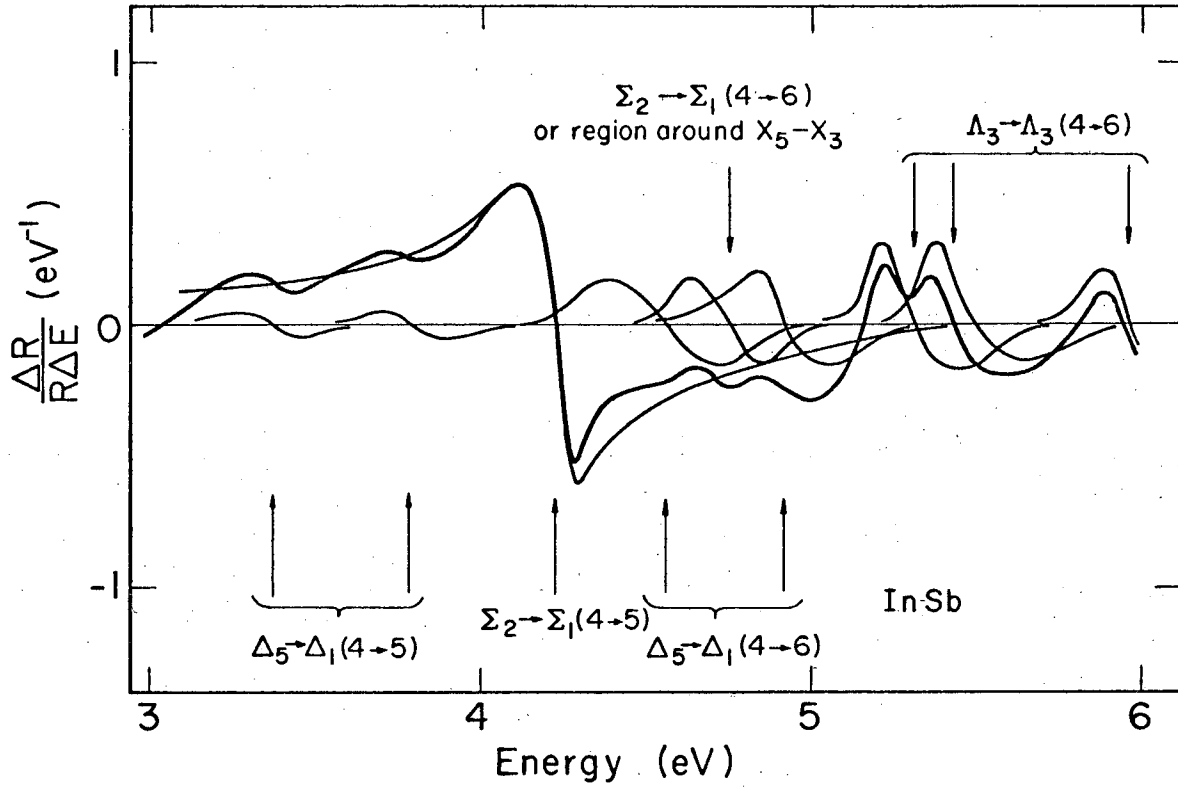
XBL699-3863

Fig. 8



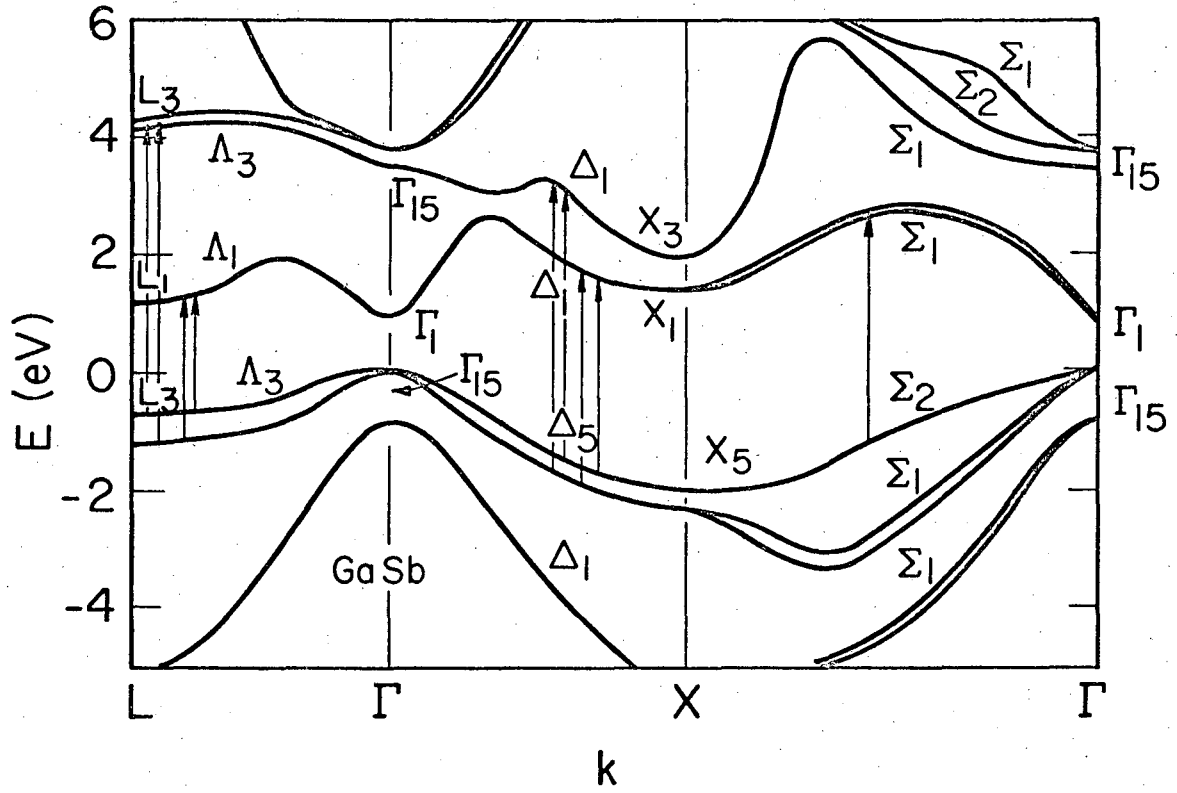
XBL699-3862

Fig. 9



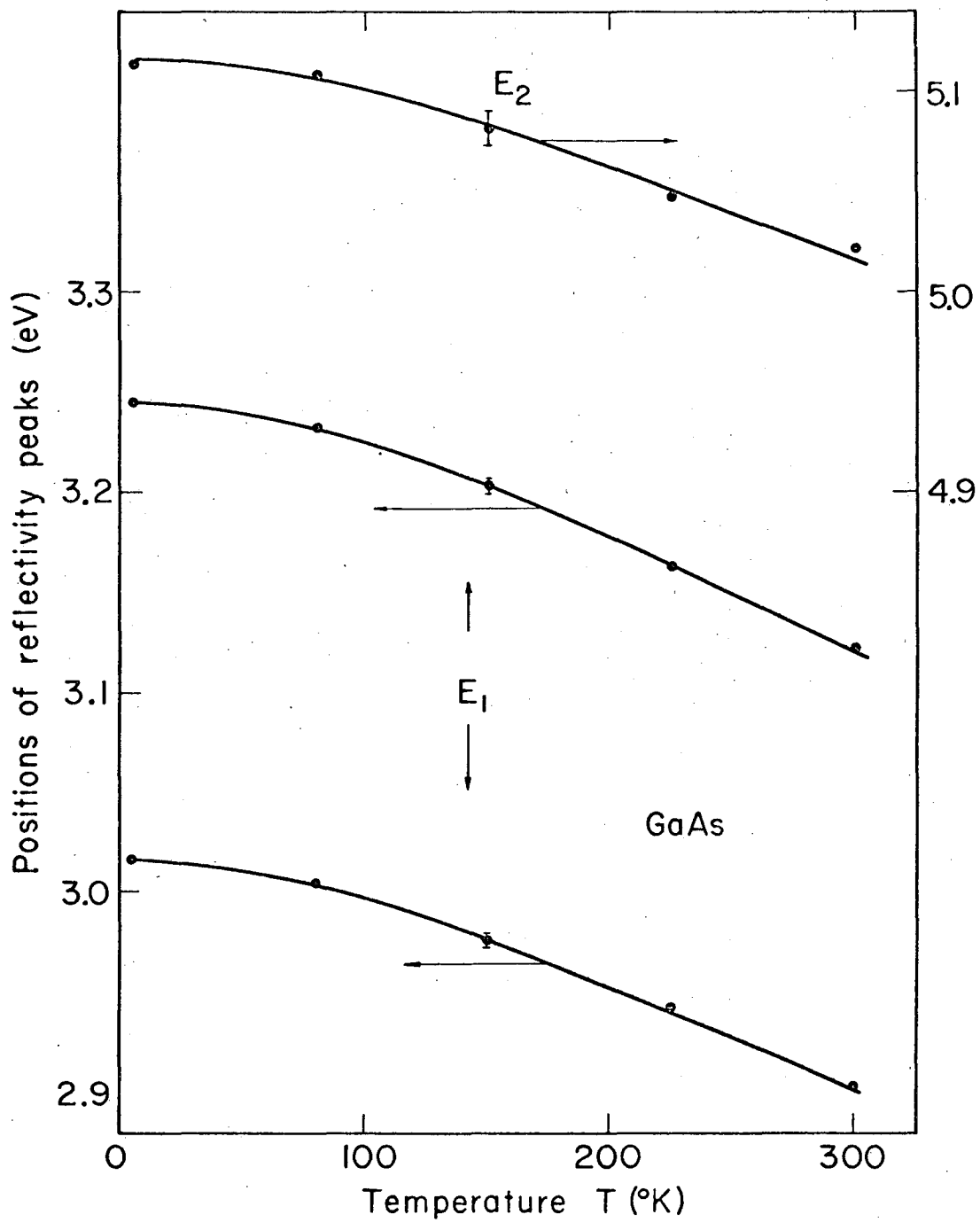
XBL699-3861

Fig. 10



XBL699-3860

Fig. 11



XBL699-3864

Fig. 12

LEGAL NOTICE

This report was prepared as an account of Government sponsored work. Neither the United States, nor the Commission, nor any person acting on behalf of the Commission:

- A. Makes any warranty or representation, expressed or implied, with respect to the accuracy, completeness, or usefulness of the information contained in this report, or that the use of any information, apparatus, method, or process disclosed in this report may not infringe privately owned rights; or*
- B. Assumes any liabilities with respect to the use of, or for damages resulting from the use of any information, apparatus, method, or process disclosed in this report.*

As used in the above, "person acting on behalf of the Commission" includes any employee or contractor of the Commission, or employee of such contractor, to the extent that such employee or contractor of the Commission, or employee of such contractor prepares, disseminates, or provides access to, any information pursuant to his employment or contract with the Commission, or his employment with such contractor.

TECHNICAL INFORMATION DIVISION
LAWRENCE RADIATION LABORATORY
UNIVERSITY OF CALIFORNIA
BERKELEY, CALIFORNIA 94720